

Magnetic properties and geochemistry of loess/paleosol sequences at Nowdeh section northeastern of Iran

Feizi, Vahid ^{*1}, Azizi, Ghasem ², Mollashahi, Maryam ³, Alimohammadian, Habib ⁴

1- Ph.D. Dep. of Geography, Climatology, Tehran University, Vahid.feizi62@gmail.com

2- Professor., Dep. of Geography, Climatology, Tehran University, ghazizi@ut.ac.ir

3- Assistant Professor of Forestry in Arid regions, Faculty of Desert Study, Semnan University,
Iranmaryam.mollashahi@semnan.ac.ir

4- Assistance Prof, Environment Magnetic Laboratory, Dep. of Geology and Mineral Exploration
halimohammadian@gmail.com

*-Corresponding Author: Feizi,Vahid. Email: vahid.feizi62@gmail.com Tell: 00989127985286

Abstract

The loess-paleosol sequences in the northeastern part of Iran serve as a high-resolution natural archive documenting climate and environmental changes. These sequences offer evidence of the interaction between the accumulation and erosion of aeolian and fluvial sediments during the Middle and Late Pleistocene periods. In this study, the Azadshar (Nowdeh Loess Section) site was chosen to reconstruct Late Quaternary climate shifts. The 24-meter thick Nowdeh loess/paleosol sequence was sampled for magnetic and geochemical analysis. The sampling involved 237 samples taken systematically at high resolution (10 cm intervals). Selected samples, corresponding to peaks in magnetic susceptibility, underwent geochemical analysis to aid in the interpretation of paleoclimatic changes indicated by the magnetic signals. The magnetic susceptibility results of the loess/paleosol deposits revealed low values during cold and dry climate periods (loess) and high values during warm and humid climate periods (paleosol). The magnetic susceptibility at a depth of 22.1 meters (approximately 130 Ka) has significantly decreased, suggesting cold climate conditions at this time. The most substantial changes in magnetic susceptibility occur at depths between 18.6 to 21.3 meters (approximately 100 to 120 Ka). During this period, there are four phases of decrease (indicating cold and dry conditions) interspersed with three phases of increase (signifying warm and humid conditions) in magnetic susceptibility. The comparison of magnetic and geochemical data showed that variations in geochemical weathering ratios corresponded to changes in magnetic parameters. A high level of correlation was observed between the magnetic susceptibility intensity and ratios such as Rb/Sr, Mn/Ti, Zr/Ti, and Mn/Sr. The findings from this research indicate that the sedimentary section of Nowdeh has experienced six distinct climate periods over the last 160,000 years. Notably, three cold and dry

periods occurred between three warm and humid periods. Additionally, during these climate phases, short-term cold (stadial) and warm (interstadial) intervals were also observed.

Keyword: Loess/paleosols sequences, Climate, Magnetic parameters, Geochemical proxies, Northeastern of Iran.

Introduction

Reconstruction of the Quaternary climate is important for the development of climate models that lead to a better understanding of past and present and prediction of future climate development. Loess–paleosol sequences are now recognized as one of the most complete terrestrial archives of glacial–interglacial climate change (Porter, 2001; Muhs and Bettis, 2003, Pierce et al, 2011, Guo et al, 2002) and have been used to reconstruct climate and geomorphological changes during the Quaternary (Karimi et al., 2011; Frechen et al., 2003; Prins et al., 2007).

Loess deposits occur in large areas of the northeast, east central, north and central parts of Iran which is part of the loess belt that covers the Middle East and extends further northward into Turkmenistan, Kazakhstan and Tajikistan (Okhravi and Amini, 2001). The extensive and thick loess deposits in northern Iran have been recently studied in detail establishing a more reliable chronological framework for the last interglacial/glacial cycle (Lateef, 1988; Pashae, 1996; Kehl et al., 2006; Frechen et al., 2009, Karimi et al, 2009, Karimi et al, 2013, Okhravi and Amini, 2001, Mehdipour et al, 2012).

Paleoclimate studies of loess deposits based on rock magnetism and combined analyses of rock magnetism and geochemistry around the world have attained appreciable advances in the past few decades (Bader et al, 2024; Jordanova and Jordanova, 2024; Heller and Liu, 1984; Forster et al., 1996; Ding et al., 2002; Guo et al., 2002; Chlachula, 2011; Bronger, 2003; Baumgart et al., 2013, Guanhua, et al, 2014). These studies comprise loess-paleosol records that cover Chinas loess plateaus, Germany, Poland, Tajikestan, Austrian, Ukraine, and the Danube catchment (Hosek et al, 2015, Ahmad and Chandra, 2013, Chen, 2010; Jordanova et al., 2011; Buggle et al., 2009; Fitzsimmons et al., 2012; Fischer et al., 2012; Jary and Ciszek, 2013; Baumgart et al., 2013; Schatz et al., 2014; Gocke et al., 2014).

Despite its suitable geographical location there is only a limited number of studies of loess deposits from the North of Iran. In this work we explore the

potential of loess deposits in northern Iran for reconstructing late quaternary climate/environmental change.

Study area

The Nowdeh section is exposed at about 20 km southeast of Gonbad-e Kavus and east of Azadshahr city. The Nowdeh river dissects a more than 24 m thick sequence of yellowish brown (10 YR 5/4) loess covering northeast dipping weathered limestone.

The study area (37° 05' 50" N and 55° 12' 58" E) is part of the Alborz structure and this structure continues beneath the Caspian Sea. This zone includes regions north of the Alborz fault and south of the Caspian Sea. Toward the east, the Gorgan-Rasht zone is covered with thick layers of loess.

The Nowdeh section was selected for this work due to earlier soil studies by Kehl et al (2005) and Frichen et al (2009) combined with the existence 12 dating for this section (Figure1).

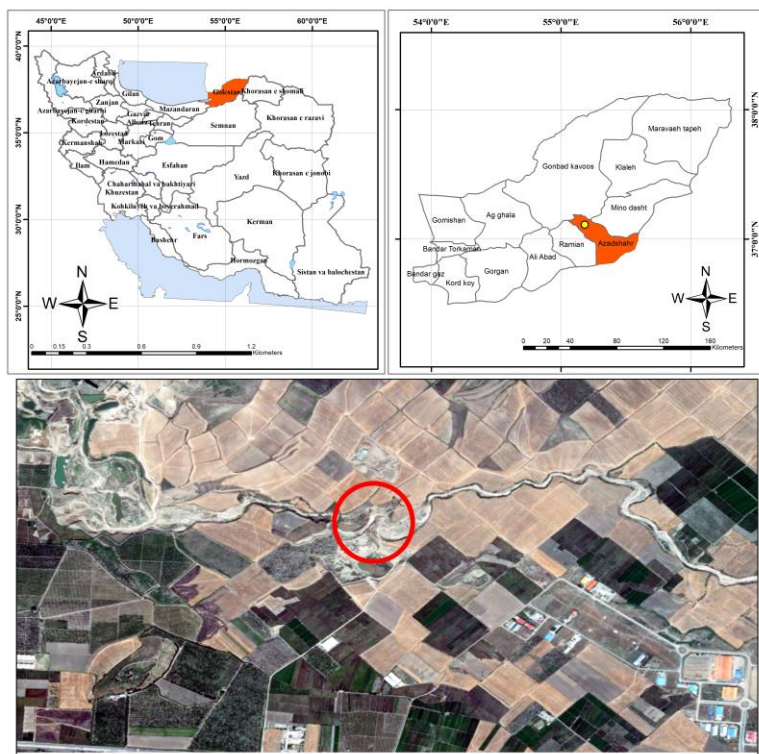


Figure 1: Map of Iran and the location of Nowdeh loess-paleosol sequence.



Figure 2: A view of the sedimentary section of the Nowdeh with its very clear layering.

Methodology

The Nowdeh loess section is approximately 24 meters thick and was sampled at 10 cm intervals for magnetometry and geochemical analysis. The sampling location and method were determined following a detailed study of the area. Magnetic susceptibility measurements of all samples were conducted at the Environmental and Paleomagnetic Laboratory of the Geological Survey of Iran in Tehran. Magnetic susceptibility is indicative of the collective response of diamagnetic, paramagnetic, ferrimagnetic, and imperfect antiferromagnetic minerals present in the samples. Each sample was placed in a 11 cm³ plastic cylinder for use in magnetic measurement devices. The measurement of magnetic susceptibility was performed using the AGICO Kappabridge model MFK1-A. To ensure the reproducibility of our results, we have meticulously documented all experimental procedures, including the setup, equipment used, and analytical methods. Our findings have been validated by testing multiple independent samples and conducting experiments repeatedly under controlled conditions.

The determination of the Saturation Isothermal Remanent Magnetization (SIRM) was carried out to assess the concentration of ferromagnetic and imperfect antiferromagnetic minerals in the samples. The calculation of the Hard Isothermal Remanence (HIRM) magnetization was performed to identify magnetically

significant components such as hematite in the samples using the following formula:

$$\text{HIRM} = 0.5(\text{SIRM} + \text{IRM} - 0.3\text{T})$$

Where $\text{IRM} - 0.3\text{T}$ is the remanence after application of a reversed field of 0.3 T after growth and measurement of SIRM. The HIRM reflects the contribution specifically of the imperfect antiferromagnetic minerals hematite and goethite (Bloemendal et al., 2008).

The $\text{S} - 0.3\text{T}$ value, or S-ratio, is calculated as

$$\text{S} - 0.3\text{T} = 0.5[(-\text{IRM} - 0.3\text{T}/\text{SIRM}) + 1]$$

and it ranges from 0 and 100%. It reflects the ratio of ferrimagnetic to imperfect antiferromagnetic minerals (Bloemendal et al., 2008).

Based on the magnetic susceptibility results, 70 samples were selected for geochemical analyses (trace elements) to assist the paleoclimatic interpretation of the magnetic signals. Each sample was washed using a sieve with a mesh size of 400 and then dried in an oven. Once dried, the samples were further sieved with a 325-mesh sieve. The very fine sediments were collected, packed, and labeled as the tested material in special containers. A 0.2-gram portion of the powder from each sample was then placed in a 1 molar hydrochloric acid solution. After two hours, the samples were analyzed using an ICP device in the laboratory. The concentrations of the main elements were measured as a percentage, while the minor elements were quantified in milligrams per kilogram. To ensure the reproducibility of the results, we meticulously document all experimental steps, including the setup, equipment used, and analysis methods. The findings of this research have been validated through the use of multiple independent samples and by conducting experiments under controlled conditions.

As explained, the studied area was previously studied by Frichen et al. (2009) and Kehl et al (2005). Therefore, we chose this sedimentary section to investigate climate changes and used their dating data. The infrared stimulated luminescence (IRSL) technique is utilized for this dating. Forty-five samples were taken in light-tight tubes for the IRSL dating study. About 250 g of sediment was sampled. Polymineral fine-graine material(4–11 mm) was prepared for the measurements. The sediment material brought on disc was irradiated by a $^{90}\text{Sr}/^{90}\text{Y}$ source in at least seven dose steps with five discs each and a radiation dose up to 750 Gy. All discs were stored at room temperature for at least 4 weeks after irradiation. The

irradiated samples were preheated for 1 min at 230 °C. De values were obtained by integrating the 1–10 s region of the IRSL decay curves. An exponential growth curve was fitted to the data and compared with the natural luminescence signal to estimate the De value. Alpha efficiency was estimated to 0.08 ± 0.02 for all samples. Dose rates were calculated from potassium, uranium and thorium contents, as measured by gamma spectrometry (Germanium detector) in the laboratory, assuming radioactive equilibrium for the decay chains. The IRSL ages gradually increase with depth from 20.5 ± 2.0 to 103 ± 10 ka. The stratigraphically oldest sample was collected below the lowermost exposed strongly developed palaeosol (PC2) at a depth of 16.10m below surface. The about 10.50 m thick loess covering the uppermost strong paleosol (PC1) likely accumulated between about 61.9 ± 6.7 and 20 ± 2.0 ka (Frechen et al, 2009).

Results Magnetic properties

In Figure 3, the relationship between susceptibility, NRM (Natural Remanent Magnetization), SIRM, HIRM, and S-0.3T in the Nowdeh section is illustrated. The variability in the magnetic susceptibility signal within the Nowdeh section indicates fluctuations in climate conditions and associated mechanisms during the Late Quaternary period. The values of magnetic susceptibility (χ) in the Nowdeh section range from 28.17 to 203.13 (in units of $10^{-8} \text{ m}^3 \text{ kg}^{-1}$). The maximum χ values (203.13) are found in the lower paleosol layer at 19.4 meters depth, while the minimum values are observed in the uppermost loess layer at 7.4 meters depth. The rock magnetic records exhibit a strong correlation with the lithology observed in the Nowdeh section. Generally, the paleosol layers exhibit higher magnetic signal intensities compared to the loess layers.

In figure 3 The paleosols exhibit higher magnetic susceptibility (χ) values compared to the loesses, with magnified magnetic enhancement observed in the Bw, Bt, and Btk horizons, while the underlying C (loess) horizon displays lower χ values. This difference probably reflects precipitation of iron oxides in the Bw horizons, resulting in a higher concentration of pedogenetic magnetite in comparison to the C horizons (Jordanova et al., 2013; Hosek et al., 2015). As illustrated in Figure 3 The χ values in the lower and middle sections of the Nowdeh profile, approximately 53-80 and 120-140 thousand years ago (Ka), (respectively at

Commented [JS1]: Please add figure reference to this paragraph

177 depths of 9 to 15 and 18 to 23 meters), represent intermediate values between
178 unweathered loesses and weathered paleosols.

179 The results indicate that the Natural Remanent Magnetization (NRM) is consistent
180 with the variance in magnetic susceptibility, particularly notable at lower depths,
181 with the highest recorded value of this parameter observed at 13.1 meters depth in
182 the BW, BWK horizon (figure 3). Variations and discrepancies in magnetic
183 susceptibility align closely with the SIRM values of the Loess sequence. As
184 magnetic susceptibility decreases, SIRM also shows a corresponding decrease. In
185 the interval between 20 to 50 thousand years ago (ka (Depth 2.1 to 8.4 meters),
186 during which much of the upper Loess formation occurred, magnetic susceptibility
187 shows minimal variation, a pattern mirrored in the SIRM diagram for this period.
188 The elevated HIRM values in Figure 3 suggest an increase in the concentration and
189 frequency of magnetic deterring minerals such as Goethite, maghemite, or
190 hematite.

191 In figure 3 The comparison between the lower values of saturation (S) (-0.3 T)
192 (between 0.6 to 0.12 Am/m) and the higher values of Hard Isothermal Remanent
193 Magnetization (HIRM) (between 2 to 5 Am/m) indicates that the proportion of
194 minerals with lower saturation, such as magnetite, is significantly lower than the
195 proportion of minerals with higher saturation in paleosols. This pattern contrasts
196 with the composition of loess deposits. As illustrated in Figure 3, This can be
197 clearly seen in loess sediments, for example, at a depth of 1 to 9 meters,
198 representing the time interval between 18 and 52 ka.

Commented [JS2]: Please add figure reference to this paragraph

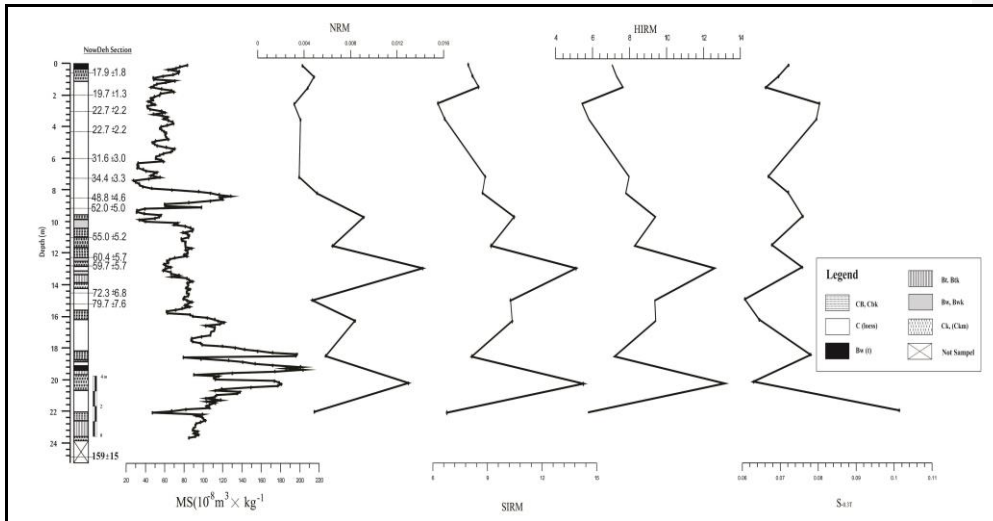


Figure 3: Basic magnetic parameters for Nowdeh section.

Element stratigraphy

Figure 4 illustrates the correlation between the concentration of selected elements (Sr, Rb, Zr, Ti, and Mn) and magnetite susceptibility in the Nowdeh section. The figure indicates significant variations in the concentration of these elements with noticeable differences between them. Sr and Rb exhibit similar trends along the Nowdeh section. At a depth of 2.9 meters, there is a notable increase in the concentration of these two elements, corresponding to an age of 22 thousand years ago (ka). Higher in the section, the concentration of Sr and Rb decreases.

In figure 4 At a depth of 18 meters, the Nowdeh sedimentary section recorded the highest concentrations of elements such as (Sr, Rb, Zr, Ti and Mn). Conversely, the lowest concentrations of these elements were observed at a depth of 8.5 meters, which dates back approximately 48, Ka.

Commented [JS3]: Please add figure reference to this paragraph

In figure 4 Ti, Zr, and Mn exhibit approximately similar trends in the diagram. These elements show little variation in concentration at the beginning of the section. The changes in element concentrations from the end of the sedimentary section down to a depth of 16.7 meters (approximately 90 ka) display a zigzag pattern. Between the depths of 16.7 and 9.3 meters, the fluctuations in element

Commented [JS4]: Please add figure reference to this paragraph

concentrations are minimal. At a depth of 9.3 meters, corresponding to roughly the last 52 ka, the research indicates the lowest concentrations of the elements measured. However, from this point onward, the concentration of elements begins to rise, peaking at a depth of 8.5 meters, which dates back about 34-48 ka. This increase suggests a period of hot and humid conditions during that time.

Commented [JS5]: Please check the age. To me this is closer to 48ka.

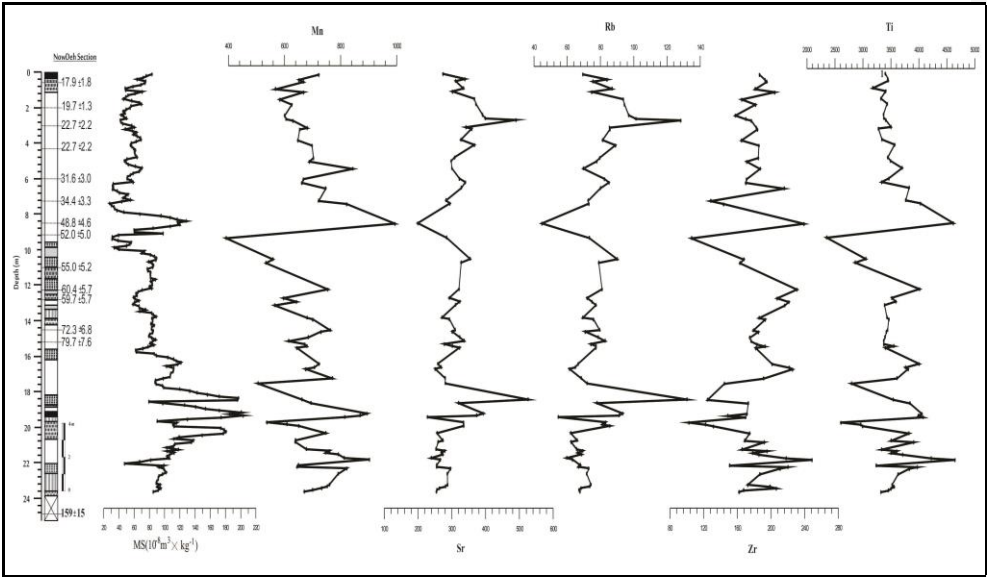


Figure 4: shows depth series of selected element concentrations for Nowdeh section.

Trace element ratio

The variation of the Si/Ti ratio in figure 5 generally follows the magnetic susceptibility pattern (figure 5), except for the lower part of the section (23-24 meters). The ratios of Mn/Sr, Zr/Ti, and Mn/Ti in figure 5 show almost no long-term change, except for at a depth of 8.5 meters, corresponding to an age of 48.8 thousand years. These changes suggest hot and humid climatic conditions, which can be correlated with the high level of magnetic susceptibility. The Rb/Sr ratio exhibits an opposite pattern to the magnetic susceptibility, especially at the depths of 8.5, 16, 19, and 22 meters. The Ba/Rb ratio generally follows the magnetic susceptibility pattern, except at depths of 13, 15, 19, and 22.8 meters where they vary oppositely.

238 The variation in the Si/Ti ratio does not exhibit a consistent relationship to the
 239 sequence of loess/palaeosol layers, as defined by the magnetic susceptibility, in the
 240 Nowdeh section. On the other hand, the Mn/Ti ratios tend to show elevated values
 241 in the palaeosols, likely due to the concentration of Mn oxide in the finer sediment
 242 fraction (Bloemendal et al., 2008). This suggests that the presence of Mn oxide
 243 plays a significant role in influencing the Mn/Ti ratio in the sediments, particularly
 244 in the palaeosol layers.

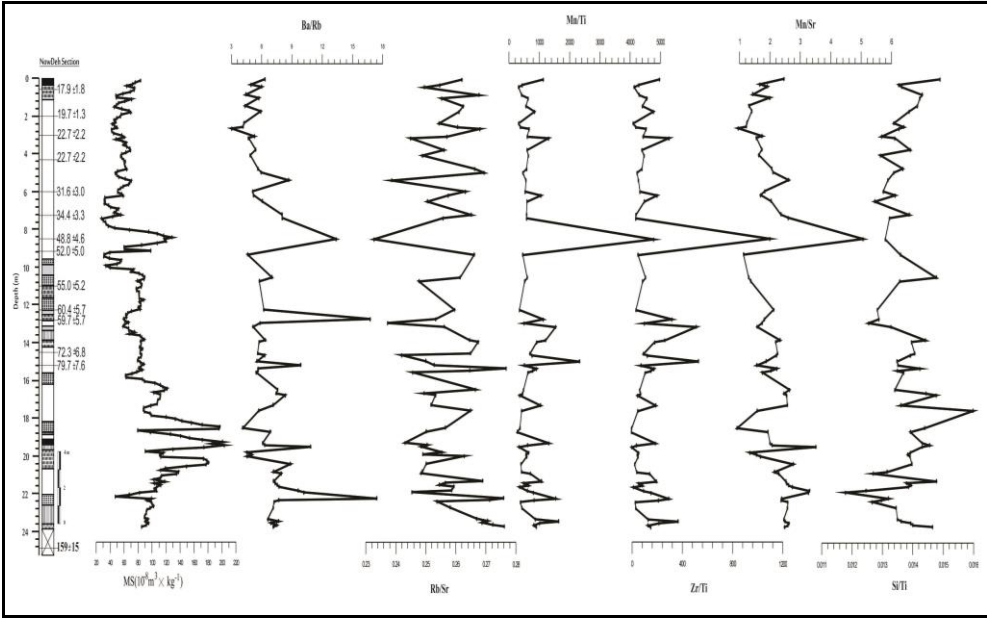


Figure 5: show selected element ratios in Nowdeh section

247 Discussion

248 Over the entire 159 Ka sequence at the Nowdeh site, there appears to be a
 249 reasonable first-order co-variation between the magnetic and geochemical
 250 indicators of weathering and soil formation, particularly with magnetic parameters
 251 reflecting variations in ferrimagnetic content and Sr-based ratios. However, upon
 252 closer detailed examination based on individual loess and palaeosol layers, an
 253 inconsistent relationship is observed between the amplitudes of individual peaks
 254 and troughs of magnetic and geochemical parameters (Fig 4 and 5). This suggests
 255 that while there is an overall correlation between these indicators at a broader
 256 scale, at a finer resolution within specific layers, the relationship becomes more

complex and inconsistent. Additional factors or processes may be influencing the variations in magnetic and geochemical parameters within the individual stratigraphic units. This issue can be seen clearly in Figures 4 and 5. As noted by Hosek et al (2015) and Makeey et al (2024), there is a significant relationship between magnetic receptivity, chemical elements, and climatic conditions. Our study reinforces this finding, as indicated by the results obtained. Recent studies have highlighted a significant relationship between climate change and the magnetic properties of sediments, indicating that alterations in sediment composition and depositional environments can reflect past climate conditions. For instance, Huang et al. (2022) demonstrated that variations in magnetic susceptibility in loess deposits are closely linked to fluctuations in moisture levels and temperature, underscoring the sensitivity of magnetic minerals to climatic changes. These findings suggest that analyzing the magnetic properties of sediments can provide valuable insights into historical climate dynamics and contribute to our understanding of how magnetic signatures may evolve in response to ongoing climate change. To investigate the relationship between climate change and the magnetic properties of sediments, we conducted magnetic susceptibility measurements on loess sediments from the Nowdeh section. The results of the magnetic susceptibility analysis demonstrated clear patterns that correlate with historical climatic fluctuations. The observed distinct sequences in magnetic susceptibility reveal insights into past environmental conditions, with lower values indicating cold and dry periods typical of loess deposition, while higher values correspond to warmer and more humid phases associated with paleosol development. These correlations between magnetic susceptibility and alternating loess-paleosol sequences provide a compelling illustration of how sediment magnetic properties reflect climatic changes over time in the Nowdeh region. The implications of these findings are significant, as they suggest that magnetic susceptibility can serve as a reliable proxy for reconstructing paleoclimatic conditions. By establishing this relationship, we enhance our understanding of how the sedimentary environment responded to climate shifts during the Pleistocene. Furthermore, these patterns of magnetic susceptibility not only inform us about specific climatic conditions but also help elucidate the feedback mechanisms between climate and weathering processes in the region. In essence, our analysis underscores the potential of magnetic susceptibility as a key indicator of past climate change, linking geological records with broader climatic events. This enhanced understanding is crucial for interpreting how similar climatic

Commented [JS6]: This part is almost purely description of results.

293 fluctuations may affect sediment dynamics in other regions with comparable loess
294 deposits.

295
296 To investigate the relationship between climate change and the magnetic properties
297 of sediments, magnetic susceptibility measurements were conducted on loess
298 sediments in the Nowdeh section. The results of the magnetic susceptibility
299 analysis at Nowdeh revealed distinct sequences corresponding to cold and dry
300 periods as well as warm and humid conditions. These variations in magnetic
301 susceptibility align with the alternating Loess paleosol sequences, indicating a
302 relationship between the magnetic properties of the sediments and past climate
303 changes in the Nowdeh region. According to Song et al. (2008), sediment loess is
304 typically formed under cold and dry climate conditions, leading to lower magnetic
305 susceptibility values due to minimal weathering processes. This observation aligns
306 with the findings in the Nowdeh section, where our data indicates that the loess
307 layers are characterized by significantly lower magnetic susceptibility than the
308 overlying paleosols. In the paleosols of the Nowdeh section, formed through
309 extensive pedogenic processes, we observe elevated magnetic susceptibility
310 attributed to increased levels of oxidation and enhanced concentrations of key
311 elements such as iron and aluminum oxides. Our magnetic susceptibility data
312 corroborate the assertion by Song et al. (2008) that paleosols generally exhibit
313 higher magnetic susceptibility compared to adjacent loess layers. Specifically, our
314 measurements indicate a distinct rise in magnetic susceptibility values within these
315 paleosols, further supporting the notion that the formation of strong magnetic
316 minerals, such as iron oxides (Fe₃O₄, γ -Fe₂O₃, and Fe₂O₃), occurs through
317 pedogenesis. Moreover, the composition of magnetic minerals in our loess samples
318 is influenced by the grain composition from the aeolian sources of sedimentation.
319 This distinction is crucial, as our data illustrates a clear contrast in magnetic
320 mineral content between the well-developed paleosols and the less altered loess
321 layers. In our analysis, we found that the paleosols not only have higher magnetic
322 susceptibility but also exhibit a more diverse range of magnetic mineral types,
323 indicating a more complex pedogenic history. This relationship highlights the
324 importance of understanding the processes of magnetic mineral formation and
325 alteration in determining the magnetic susceptibility profiles of sediment
326 sequences. Our own findings reinforce the established understanding from previous

Commented [JS7]: This part is mostly describing results.

studies, such as those by Song et al. (2008), while providing new insights into the specific conditions and processes at play in the Nowdeh section.

According to Song et al. (2008), sediment loess is formed under cold and dry climate conditions, leading to lower magnetic susceptibility due to the absence of significant weathering processes. In contrast, in paleosols formed as a result of pedogenic processes, the level of oxidation increases, resulting in an increase in magnetic susceptibility records due to higher concentrations of XYZ elements. It is widely observed, that in a loess/paleosol sequence, paleosols exhibit higher magnetic susceptibility than the adjacent loess layers (Song et al., 2008). The formation of strong magnetic minerals, such as iron oxides, in soils through pedogenesis processes includes minerals like Fe_3O_4 , $\gamma\text{-Fe}_2\text{O}_3$, and $\alpha\text{-Fe}_2\text{O}_3$. In contrast, the mineral magnetism of loess layers is influenced by the grain composition of the aeolian sources depositing the sediments. This distinction in magnetic mineral content between soils undergoing pedogenesis and loess layers sourced from aeolian deposits contributes to the differences in magnetic susceptibility observed between paleosols and loess layers in sediment sequences. In Fig. 3, the brown layer sequences of dark and light paleosols within the loess deposits illustrate distinct weathering processes that reflect the climatic patterns observed during glacial and interglacial periods of the middle and late Pleistocene. The higher magnetic susceptibility of the paleosols compared to the surrounding loess layers indicates a significant degree of pedogenesis and oxidation, consistent with findings by Maher (2011) and Spassov (2002). This difference is particularly pronounced at lower depths, suggesting that these layers experienced greater weathering variability during those periods. At a depth of 21 meters (approximately 110 ka), the notable decrease in magnetic susceptibility suggests a transition to colder and drier conditions, which aligns with the known climatic shifts of that era. This finding is crucial because it highlights how magnetic susceptibility can serve as a proxy for past climatic conditions, providing insights into the environmental changes that influenced soil development (Thompson & Oldfield, 2021; Liu et al., 2022). The magnetic susceptibility chart for the Nowdeh section reveals around eight distinct periods of increasing magnetic susceptibility, indicative of elevated temperatures and humidity, consistent with findings from other regions that link magnetic properties to climatic variations (Dearing et al., 2023; Heller & Liu, 2020). The magnetic susceptibility chart for the Nowdeh section reveals around eight distinct periods of increasing magnetic susceptibility, indicative of elevated

Commented [JS8]: ??? Not sure what is meant here.

Commented [JS9]: This section lacks relation with your own data. You are discussing magnetic susceptibility without informing the reader how this is related to your work.

temperatures and humidity. This pattern suggests a correlation between magnetic susceptibility and climatic conditions, where periods of increased susceptibility correspond to warmer, more humid phases conducive to soil formation.

Commented [SJ10]: Additional references possible here?

In Fig 3, the brown layer sequences of dark and light paleosols in the loess deposits demonstrate distinct weathering processes that closely resemble the patterns observed during glacial and interglacial periods in the middle and late Pleistocene. The paleosols in the Nowdeh section exhibit higher magnetic susceptibility compared to the surrounding loess layers. This difference is more prominent at lower depths, indicating greater weathering variability during those periods. At a depth of 21 meters (Almost 110 ka), a significant decrease in magnetic susceptibility suggests a cold and dry condition during that timeframe. The magnetic susceptibility chart for the Nowdeh section reveals approximately 8 distinct periods of increasing magnetic susceptibility, reflecting periods of temperature and humidity elevation.

In accordance with the standard global loess characteristics, paleosols consistently exhibit higher magnetic susceptibility values compared to adjacent loess layers due to pedogenesis and oxidation processes, as highlighted by Maher (2011) and Spassov (2002). The NRM results suggest a decrease during loess formation and an increase during paleosol formation (figure 3). This pattern suggests a relationship between NRM and magnetic susceptibility figure 3 (Bloemendal et al, 2008,). A decrease in NRM indicates dry and cold Climate conditions in figure 3 (The depth of 7.2 meters, which is approximately equal to 34 Ka), consistent with the deposition of loess layers, while an increase in NRM represents warmer and more humid Climate-climate conditions, corresponding to paleosol formation. The results presented in the previous section illuminate the significant relationship between NRM (Natural Remanent Magnetization) and magnetic susceptibility, contributing to our understanding of past climatic conditions. The observed decrease in NRM at a depth of 7.2 meters (approximately 34 ka) is indicative of drier and colder climate conditions, consistent with the processes associated with loess deposition. This finding reinforces the notion that periods of extensive loess accumulation correspond with colder climatic phases, as seen in other studies of similar stratigraphic sequences. Conversely, the increase in NRM at depths of 18.6 to 21.3 meters marks a shift toward warmer and more humid conditions, which correlates with paleosol formation. This transitional phase highlights the dynamic interplay between climate and soil development, suggesting that optimum

Commented [JS11]: This section almost exclusively describes results

Commented [JS12]: Please add figure reference here.

Commented [JS13]: Please add figure reference here. It is very difficult to have too many figure references. It is easy, however, to not have enough.

conditions for soil formation fostered the development of paleosols during this time. The highest magnetic susceptibility values in this layer, documented in Fig. 3, further corroborate the enhancing environmental conditions during this interval. The peak alignment of NRM and magnetic susceptibility at a depth of 19.4 meters, and approximately 120 ka, is particularly noteworthy. This correlation may signify a period of climatic stability that allowed for the establishment of rich soil profiles, crucial for understanding the ecological dynamics at play during the late Pleistocene. Such findings align with previous research by Bloemendal et al. (2008), which also emphasized the relevance of magnetic properties in interpreting paleoclimatic conditions.

The probable justifications for the low alteration in magnetic susceptibility and isothermal remnant magnetization between 20 to 50 thousand-Ka(Figure 3) years ago can be attributed to two main factors:

- 1- Decreased Pedogenesis due to cold and dry periods.
- 2- Reduction in the influx of magnetic particles into loess layers.

During the last 20 ka, there seems to be a correlation between magnetic susceptibility variations in the surface soil layer and climatic conditions. This period coincides with the transition from cold Climate to the current warm and humid climate in the northern region of Iran (Frichen et al, 2009). As a result, the soil's magnetic properties, specifically the saturation isothermal remanent magnetization (SIRM), have likely increased during this time frame. However, since the SIRM samples were only collected at magnetic susceptibility peak points, they may not capture the full extent of variations. Comparing these findings with the research by Antoine et al. (2013) on loess/paleosol sediments in Central Europe reveals a close relationship, particularly around 32 ka. The close relationship observed in our findings and those of Antoine et al. around 32 ka suggests a synchronous response of the magnetic susceptibility of sediments to environmental changes during this period. This synchrony reinforces the idea that widespread climatic or geological factors were influencing sediment formation across regions. Also, Antoine et al. provided critical insights into the paleoenvironmental conditions in Central Europe during the Late Pleistocene.

Geochemical charts can serve as useful indicators of Climate patterns, as they can highlight different levels of weathering severity. In the study of loess deposits, certain chemical ratios can be utilized to reconstruct variations in paleoclimate

Formatted: Space After: 1.6 pt

Commented [JS14]: Please add figure reference.

Formatted: Indent: Before: 0", First line: 0", Tab stops: 0", Left

Commented [JS15]: Would it be useful to say something about the wider implications of this close relationship? Similar signal across large regions.

(Ding et al., 2001). The Zr/Ti, Mn/Ti, Rb/Sr, and Mn/Sr records from the Nowdeh section exhibit a clear pattern of higher values prevailing in the palaeosols, and their high degree of similarity is noteworthy. Rb/Sr has been suggested by several researchers as an indicator of pedogenic intensity in loess, based on the differential weathering of the major host minerals, specifically K-feldspar for Rb and carbonates for Sr (Hosek et al, 2015, makeey et al, 2024). In the case of Mn/Sr, the higher values observed in the palaeosols are likely a result of the combined effects of grain size on Mn concentration, as well as the loss of Sr through solution processes. This indicates that these ratios can serve as important indicators of pedogenic processes and weathering dynamics in the sedimentary record of the Nowdeh section. Rubidium is derived from K-feldspar, while strontium comes from carbonate minerals. As soils weather, an increase in Rb/Sr often indicates selective retention of Rb while Sr is leached away, reflecting greater weathering intensity (Bai et al., 2022). Climate-driven changes, such as increased precipitation, can enhance Sr leaching, leading to higher Rb/Sr ratios in wetter conditions. This relationship highlights how climate influences elemental cycling in soils (Zhang et al., 2021).

Commented [JS16]: This would be good start to this paragraph. You do briefly indicate the aspect you want to discuss (please make sure that this finding is also described in the results).

Commented [JS17]: This part is an interpretation of the finding introduced in the previous sentence, which is good. You can embed the Ding work in this part of the paragraph, but it should have a more direct relation to your data (e.g. how specifically are specific ratios affected by climate change pattern enabling using those ratios to deduce climate change).

The magnetic susceptibility record shows high values at a depth of 19.4 meters has recorded high values, which indicates indicating the hot and humid climate conditions at this depth with an prevailing around approximate age of 120 ka age. Variations in the concentrations of manganese (Mn), zirconium (Zr), and titanium (Ti) in the soil reflect a clear stratigraphic pattern (figure 4), with higher values seen in paleosols and lower values in the loess layers (Bloemendal et al., 2008). This pattern is influenced, in part, by carbonate dilution/concentration effects, as a significant portion of the variability in these elements disappears when expressed on a carbonate-corrected basis. In a study by Chen et al. (1999), a comparison was made between the Rb/Sr ratios and magnetic susceptibility values in the uppermost (last glacial/interglacial) sections of the Luochuan and Huanxian regions. The researchers noted a remarkable correspondence between the amplitudes of variation in magnetic susceptibility and Rb/Sr ratios. This finding suggests a close relationship between magnetic susceptibility variations and the Rb/Sr ratios in these regions during the last glacial and interglacial periods. Magnetic susceptibility at a depth of 19.4 meters has recorded high values, which indicates the hot and humid climate conditions at this depth with an approximate age of 120

Commented [JS18]: As another example, this would be a good start to this paragraph. The Chen work could then be used to start interpretation of your results, in conjunction with the Bloemendal work.

Commented [SJ19]: Figure reference missing

ka. Variations in the concentrations of manganese (Mn), zirconium (Zr), and titanium (Ti) in the soil reflect a clear stratigraphic pattern, with higher values seen in paleosols and lower values in the loess layers (Bloemendal et al., 2008). This pattern is influenced, in part, by carbonate dilution/concentration effects, as a significant portion of the variability in these elements disappears when expressed on a carbonate corrected basis.

In the Nowdeh section, the amount of rubidium (Rb) in paleosols was lower compared to its concentration in loess layers (Figure 5). This discrepancy can be attributed to the higher solubility of Rb in warm and humid climates, typical of interglacial periods. Gallet et al. (1996) observed significant depletion of Rb in the paleosols, supporting this interpretation. Recent research by Zhu et al. (2021) demonstrated that climate change alters the biogeochemical cycling of nutrients, including Rb, leading to increased leaching in saturated soils during periods of heavy rainfall. Additionally, studies by Arias-Ortiz et al. (2020) highlighted that changing climate conditions contribute to shifts in soil chemistry and nutrient availability, affecting soil formation and stability. Their findings underline the complex interactions between climate variations and elemental behavior in soil profiles. Furthermore, a comprehensive review by Jiang et al. (2020) emphasized the impacts of climate change on soil properties, particularly focusing on leaching processes and the resultant changes in nutrient concentration due to increased precipitation and temperature.

Our results indicate that the Mn/Ti, Zr/Ti, and Mn/Sr ratios tend to exhibit higher values in the paleosols. According to Ding et al. (2001), elevated Mn/Ti values in paleosols may result from the concentration of iron (Fe) and manganese (Mn) oxides in the finer sediment fractions. They also noted that the Rb/Sr and Mn/Sr ratios show a clear pattern of elevation in the paleosols, which aligns with the findings of our study (figure 5). The Rb/Sr ratio has been proposed by various researchers as an indicator of pedogenic intensity in loess deposits, based on the differential weathering of major host minerals such as K-feldspar for Rb and carbonates for Sr. The higher Mn/Sr values in paleosols may be attributed to grain-size effects on Mn concentrations and the solubilization loss of Sr.

Chen et al. (1999) compared Rb/Sr and magnetic susceptibility in the uppermost parts of the Luochuan and Huanxian sections, revealing a significant correspondence between the variations in magnetic susceptibility and Rb/Sr ratios. This suggests a link between weathering intensity and magnetic properties in these

Commented [JS20]: As another example, this would be a good start to this paragraph. The Chen work could then be used to start interpretation of your results, in conjunction with the Bloemendal work.

Commented [JS21]: Please add figure reference.

Commented [JS22]: This paragraph is good example of what is missing. You do start well by outlining a piece of your results. This is followed by stating your interpretation, without really justifying it. Is there for example a process described in the Gallet work that helps explaining this pattern. Have other people used such data in a similar way?

Commented [SJ23]: Figure ref

sediments. In the context of the Nowdeh sedimentary section, the magnetic parameters were compared with those from other studies conducted in various regions of the world, further contributing to our understanding of paleoclimatic variations and weathering processes in loess deposits.

In figure 6 The comparison of magnetic receptivity results from the Nowdeh sedimentary section with the palynological data from sedimentary cores of Urmia Lake (Djamali et al., 2008) and the ^{18}O analysis from Arabian Sea sedimentary cores (Tzedakis, 1994) has provided valuable insights into past climate conditions (Figure 6). In the analysis, an increase in the AP/NAP index (Arboreal Pollen grains (AP) to that of the Non-Arboreal Pollen grains (NAP)) in the lakes corresponded with the presence of ancient soil layers in the seedling sedimentary section.

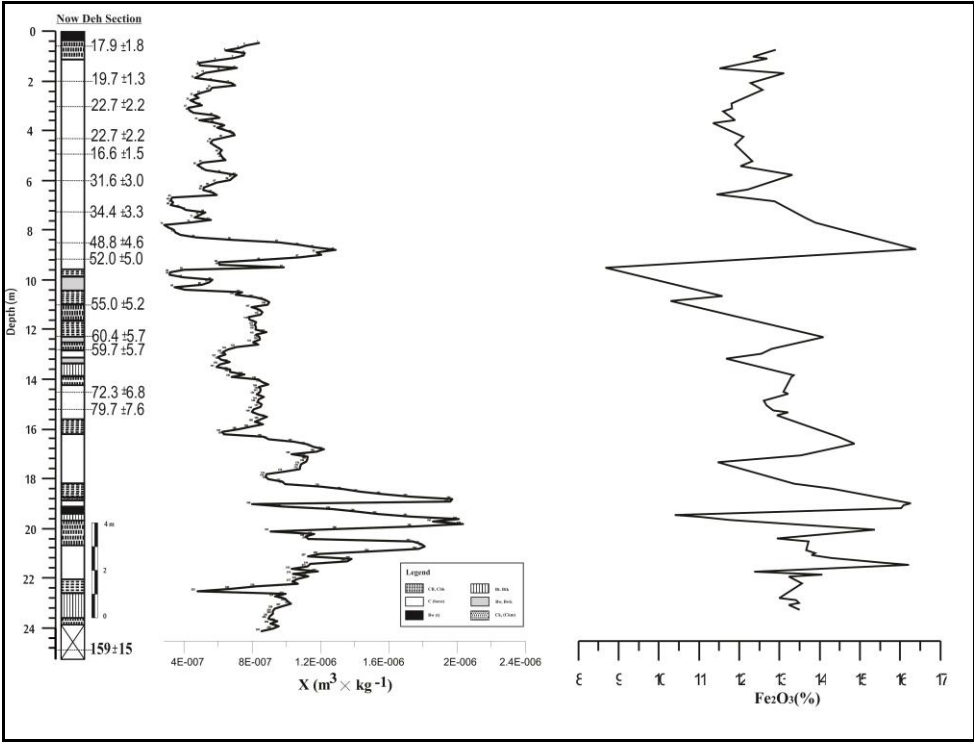
This increase signifies warmer temperatures and higher humidity levels, conducive to the growth of trees and shrubs (Harrison et al., 2020; Zhang et al., 2021). Conversely, a decrease in the AP/NAP index indicates a decline in temperature and humidity, leading to the disappearance of trees and shrubs and changes in surface vegetation cover (Chen et al., 2022). This correlation suggests that the climate conditions and their fluctuations in western Iran align with the sedimentary deposition at Nowdeh, consistent with findings from similar studies in the region (Fuchs et al., 2013; Hosek et al., 2015).~~This increase signifies warmer temperatures and higher humidity levels, conducive to the growth of trees and shrubs. Conversely, a decrease in the AP/NAP index indicates a decline in temperature and humidity, leading to the disappearance of trees and shrubs and changes in surface vegetation cover. This correlation suggests that the climate conditions and their fluctuations in western Iran align with the sedimentary deposition at Nowdeh.~~

Moreover, in figure 6 the ^{18}O analysis of the Arabian Sea exhibited a strong agreement with magnetic receptivity data. A decrease in the ^{18}O indexes points to warmer climate conditions, while an increase indicates colder conditions (Djamali et al, 2008). The relationship between magnetic susceptibility and ^{18}O levels in the Arabian Sea sediments, as shown in Figure 6, Verify that an increase in magnetic susceptibility corresponds with a decrease in ^{18}O levels, indicating warmer climate conditions. This alignment further supports the connection between the recorded palynology data of Lake Urmia, ^{18}O data from the Arabian Sea, and the sequence of ancient loess-soil sediments in the Nowdeh sedimentary section.

Commented [SJ24]: Please add more references - in this section but also more generally in the discussion

Commented [SJ25]: Please add figure reference. As a general rule, please add a figure reference whenever you are referring to a finding in your work. It is rather difficult to have too many figure references, but it is easy to not have enough.

556 intervals. This issue can also be seen in the amount of Fe_2O_3 in Nowdeh sediments
 557 (Figure 7). While the older sediments also show a significant association with
 558 climate variations in Central Europe and the Nowdeh area, the absence of
 559 radiometric dating in these older sediments introduces some uncertainty when
 560 interpreting these findings. Nonetheless, the consistent patterns in magnetic
 561 susceptibility across different time periods provide valuable insights into past
 562 climate fluctuations and their impact on soil properties in these regions.



563
 564 Figure 7: The relationship between magnetic susceptibility and Fe_2O_3

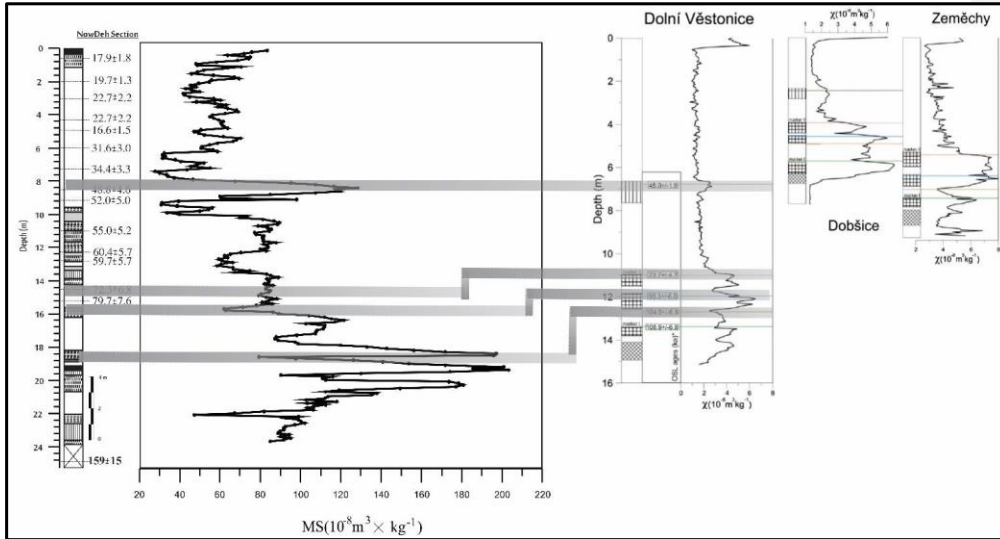


Figure 8: Comparison of changes in magnetic receptivity of Dolní Věstonice sedimentary section, Fuchs et al, 2013, Dobšice and Zemechy section, Hošek et al, 2015, with Nowdeh sedimentary section

The comparison of magnetic receptivity trends as recorded in sedimentary sections of Beiyuan, Heimugou, Biampo, and the ^{18}O records by Imbrie et al. (1984) in Figure 8 reveals a high agreement with the Nowdeh sedimentary section. This alignment indicates similar Climate conditions across different locations in the Northern Hemisphere.

The consistency in magnetic receptivity trends among these various sites suggests a commonality in the climatic conditions experienced during the corresponding time periods. This synchronization in magnetic susceptibility patterns further supports the notion that these regions were subjected to comparable environmental changes and fluctuations in the past.

Additionally, the correlation observed between the magnetic receptivity data and the ^{18}O records underscore the close relationship between climatic factors and sedimentary deposition patterns across these sites (Figure 9). By examining these geological proxies, researchers can gain valuable insights into the past climate dynamics and variations that have affected the Northern Hemisphere over time.

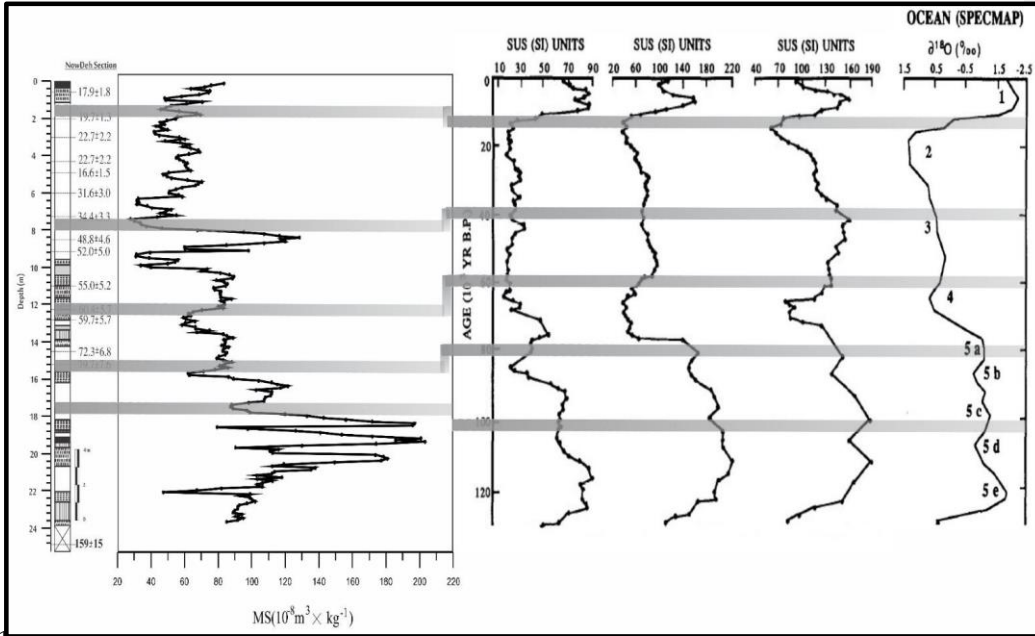


Figure 9: Comparison of magnetic receptivity changes of Beiyuan, Heimugou, Biampo, An et al, 1991, records of ^{18}O Imbrie et al, 1984 with Nowdeh sedimentary section

The findings of Mehdipour et al. in 2012 in the realm of fine loess exhibit a close resemblance to the results presented in our research, as illustrated in Figure 9. In their study, they employed both magnetic and geochemical approaches to assess different climatic periods, and the outcomes align significantly with the findings of Our research. The comparison in Figure 10 reveals a strong consistency in the magnetic receptivity trends between the Nowdeh section and the Neka sedimentary section analyzed by Mehdipour et al (2012). Between 48 and 20 thousand years ago, notable similarities are observed in the fluctuations of magnetic receptivity in both sedimentary sections. Whenever there is an increase in magnetic receptivity, it indicates a warm and humid period with the formation of ancient soil layers. This shared pattern implies a synchrony in climatic conditions between the two regions during this time frame, showcasing the utility of magnetic susceptibility as a proxy for understanding past environmental changes and soil development processes.

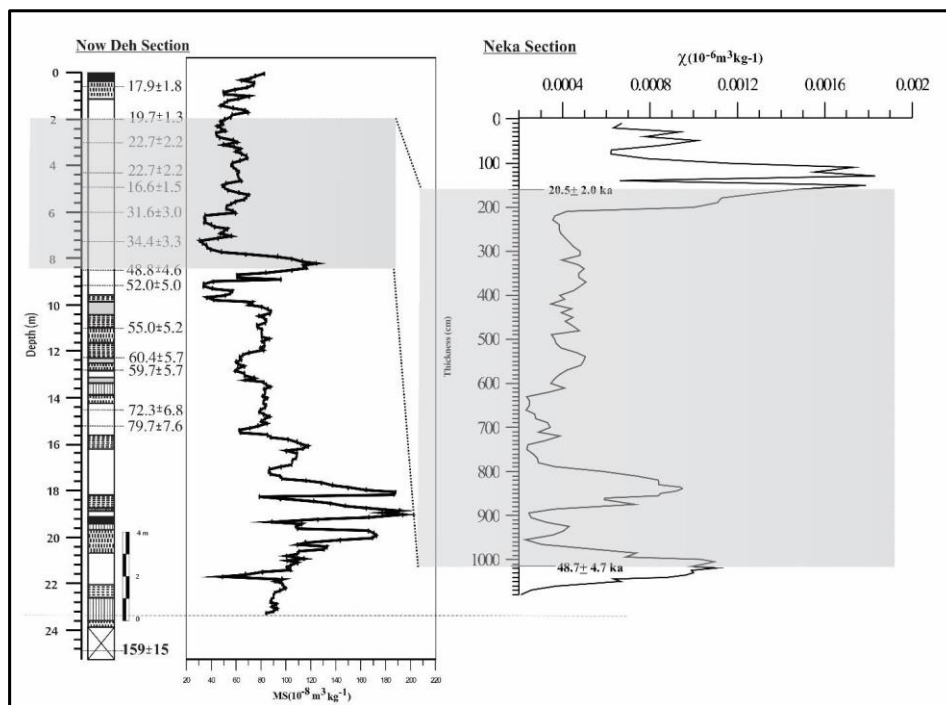


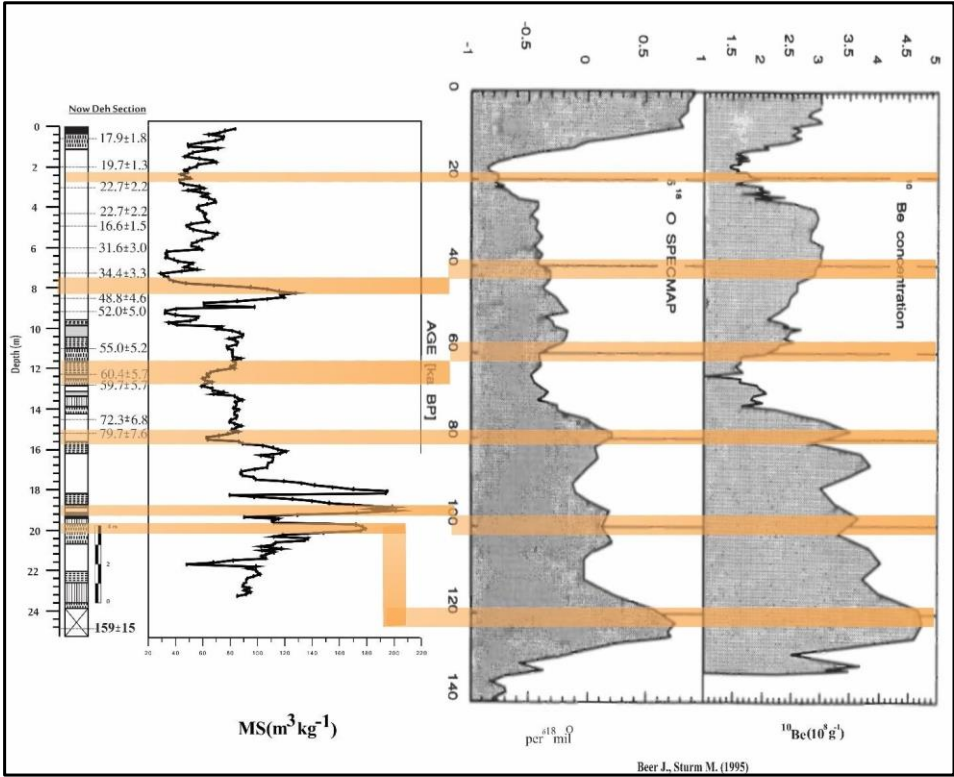
Figure 10: Comparison of magnetic receptivity diagram of Nowdeh sedimentary section with Neka sedimentary section (Mahdi et al., 2012)

The results of this research exhibit a strong consistency with the findings of Beer and Sturm (1995) regarding beryllium saturation in the Zaifang sedimentary section and ^{18}O in marine sediments. In both cases, there is a clear correlation between the fluctuations in beryllium saturation, ^{18}O , and magnetic receptivity.

When beryllium saturation and ^{18}O decrease, there is a corresponding decrease in magnetic receptivity, indicating colder and drier climate conditions. Conversely, an increase in beryllium saturation and ^{18}O is accompanied by an increase in magnetic receptivity, signifying warmer and more humid periods.

The high agreement between the climatic periods identified based on these parameters in the Zaifang sedimentary section and marine sediments, and the magnetic receptivity trends observed in the Nowdeh sedimentary section, highlights the synchrony of similar climate events in the past across different locations. This consistency further supports the robustness of magnetic

617 susceptibility as a proxy for understanding past climate variations and
618 environmental changes (figure 11).



619
620 Figure 11: Comparison of magnetic receptivity results of Nowdeh sedimentary section in comparison with
621 ^{18}O and Be 10 isotope results of Xifeng sedimentary section (Beer and Sturm, 1995).

622
623 **Conclusion**

624 In conclusion, the loess/paleosol sequences from Northeastern Iran serve as a
625 valuable archive for studying the paleoenvironmental changes during the Upper
626 Pleistocene. By employing a multi-proxy approach that integrates
627 sedimentological, magnetic, and geochemical methods, the following key insights
628 have been revealed:

1. The stratigraphy of the studied section aligns well with the typical pattern of Upper Pleistocene loess/paleosol successions in the region, providing valuable insights into the past environmental conditions.
2. Magnetic parameters show a strong correlation with climate conditions, making them effective variables for reconstructing climate change patterns in the region.
3. Comparisons between magnetic and geochemical data indicate that variations in geochemical weathering ratios mirror changes in magnetic weathering parameters, such as magnetic susceptibility, further enhancing our understanding of past environmental dynamics.
4. The high degree of coherence observed between the amplitudes of magnetic susceptibility and various geochemical ratios, including Rb/Sr, Mn/Ti, Zr/Ti, and Mn/Sr, reinforces the reliability of magnetic susceptibility as a proxy for tracking environmental changes and provides additional insights into the interplay between magnetic and geochemical processes.

Overall, this comprehensive multi-proxy analysis enhances our understanding of the paleoenvironmental changes in Northeastern Iran during the Upper Pleistocene period and emphasizes the importance of integrating sedimentological, magnetic, and geochemical data to unravel past climatic fluctuations and environmental dynamics.

References

1. Ahmad, I., Chandra, R., 2013, Geochemistry of loess-paleosol sediments of Kashmir Valley, India: Provenance and weathering, *Journal of Asian Earth Sciences* 66, 73-89.
2. Antoine, P., Rousseau, D.D., Degeai, J.P., Moine, O., Lagroix, O., Kreutzer, S., Fuchs, M., Hatte, C.H., Gauthier, C., Svoboda, J. and Lisa, I., 2013, High-resolution record of the environmental response to climatic variations during the Last Interglacial Glacial cycle in Central Europe: the loess-palaeosol sequence of Dolní Věstonice (Czech Republic), *Quaternary Science Reviews*, 67, PP 17-38.
3. Arias-Ortiz, A., et al. (2020). "The impact of climate change on soil chemistry and biogeochemical cycles." *Nature Reviews Earth & Environment*, 1(12), 689-702.
4. Bader N E, Broze E A, Coates M A, Elliott M M, McGann G E, Strozyk S, Burmester R F, 2024, The usefulness of the magnetic susceptibility of loess paleosol sequences for paleoclimate and stratigraphic studies: The case of the Quaternary Palouse loess, northwestern United States, *Quaternary International*, Article in Press.
5. Bai, Y., et al. (2022). "Rb/Sr ratio as a proxy for weathering and soil formation in the Loess Plateau, China." *Geoderma*, 410, 115754.

6. Baumgart, P., Hambach, U., Meszner, S., Faust, D., 2013. An environmental magnetic fingerprint of periglacial loess: records of Late Pleistocene loess paleosol sequences from Eastern Germany. *Quat. Int.* 296, 82–93.
7. Bloemendal J, Liu X, Sun Y, Li N, 2008, An assessment of magnetic and geochemical indicators of weathering and pedogenesis at two contrasting sites on the Chinese Loess plateau, *Palaeogeography, Palaeoclimatology, Palaeoecology* 257 (2008) 152–168.
8. Bloemendal, J., Xiuming L., Youbin, S., Ningning L., 2008. An assessment of magnetic and geochemical indicators of weathering and pedogenesis at two contrasting sites on the Chinese Loess plateau, *Palaeogeography, Palaeoclimatology, Palaeoecology* 257; 152–168.
9. Bronger, A., 2003. Correlation of loess-paleosol sequence in East and Central Asia with SE Central Europe: toward a continental Quaternary pedostratigraphy and paleoclimate history. *Quaternary International* 106/107, 11–31.
10. Buggle, B., Hambach, U., Glaser, B., Gerasimenko, N., Markovic, S., Glaser, I., Zöller, L., 2009. Stratigraphy, and spatial and temporal paleoclimatic trends in Southeastern/Eastern European loess–paleosol sequences. *Quat. Int.* 196, 186–206.
11. Chen, J., An, Z.S., Head, J., 1999. Variation of Rb/Sr ratios in the loess–paleosol sequences of central China during the last 130,000 years and their implications for monsoon paleoclimatology. *Quaternary Research* 51, 215–219.
12. Chen, T., Xie, Q., Xu, H., Chen, J., Ji, J., Lu, J., Lu, H and Balsam, W., 2010. Characteristics and formation mechanism of pedogenic hematite in Quaternary Chinese loess and paleosols, *Catena* 81, 217–225.
13. Chen, Y., Wang, X., & Li, J. (2022). Impact of climate fluctuations on vegetation patterns in arid regions: Case study from northwestern China. *Quaternary Science Reviews*, 265, 106552.
14. Chlachula, J., Little, E., 2011. A high-resolution Late Quaternary climatostratigraphic record from Iskitim, Priobie Loess Plateau, SW Siberia, *Quaternary International* 240, 139e149
15. Ding, Z.L., Ranov, V., Yang, S.L., Finaev, A., Han, J.M., Wang, G.A., 2002. The loess record in southern Tajikistan and correlation with Chinese loess. *Earth and Planetary Science Letters* 200, 387e400.
16. Ding, Z.L., Yang, S.L., Sun, J.M., Liu, T.S., 2001. Iron geochemistry of loess and Red Clay deposits in the Chinese Loess Plateau and implications for long-term Asian monsoon evolution in the last 7.0 Ma. *Earth and Planetary Science Letters* 185, 99–109.
17. Fischer, P., Hilgers, A., Protze, J., Kels, H., Lehmkuhl, F., Gerlach, R., 2012. Formation and geochronology of Last Interglacial to Lower Weichselian loess/palaeosol sequences — case studies from the Lower Rhine Embayment, Germany. *E & G Quat.Sci. J.* 61, 48–63.
18. Fitzsimmons, K.E., Marković, S.B., Hambach, U., 2012. Pleistocene environmental dynamics recorded in the loess of the middle and lower Danube Basin. *Quat. Sci. Rev.* 41,104–118.
19. Forster, T., Evans, M.E., Havlíček, P., Heller, F., 1996. Loess in the Czech Republic:magnetic properties and paleoclimate. *Stud. Geophys. Geod.* 40, 243–261.
20. Frechen, M., Kehl, M., Rolf, C., Sarvati, R., Skowronek A., 2009, Loess Chronology of the Caspian Lowland in Northern Iran, *Quaternary International*, No. 198, pp. 220-233.

Formatted: Indent: Hanging: 0.25"

21. Frechen, M., Oches, E.A., Kohfeld, K.E., 2003. Loess in Europe—mass accumulation rates during the Last Glacial Period. *Quaternary Science Reviews* 22, 1835–1875.
22. Gallet, S., Jahn, B.M., Torii, M., 1996. Geochemical characterization of the Luochuan loess-paleosol sequence, China, and paleoclimatic implications. *Chemical Geology* 133, 67–88.
23. Gocke, M., Hambach, U., Eckmeier, E., Schwark, L., Zöller, L., Fuchs, M., Löscher, M., Wiesenberg, G.L.B., 2014. Introducing an improved multi-proxy approach for paleoenvironmental reconstruction of loess–paleosol archives applied on the Late Pleistocene Nussloch sequence (SW Germany). *Palaeogeogr. Palaeoclimatol. Palaeoecol.* 410, 300–315.
24. Guanhua, L., Dunsheng, X., Ming, J., Jia, J., Jiabo, L., Shuang Z., Yanglei, W., 2014. Magnetic characteristics of loess/paleosol sequences in Tacheng, northwestern China, and their paleoenvironmental implications. *Quaternary International*, 3, 1–10.
25. Guo, Z.T., Ruddiman, W.F., Hao, Q.Z., Wu, H.B., Qiao, Y.S., Zhu, R.X., Peng, S.Z., Wei, J.J., Yuan, B.Y., and Liu, T.S., 2002. Onset of Asian desertification by 22 Myr ago inferred from loess deposit in China. *Nature* Vol. 416, pp. 159–163.
26. Harrison, S. P., Prentice, I. C., & Baird, A. J. (2020). Vegetation and climate change: Implications for ecosystem services. *Global Change Biology*, 26(2), 429–445.
27. Heller, F., Liu, T., 1984. Magnetism of Chinese loess deposits. *Geophys. J. R. Astron. Soc.* 77, 125–141.
28. Hosek J., Hambach U., Lisa L., Grygar T.M., Horacek I., Meszner S., Knesl I., 2015. An integrated rock-magnetic and geochemical approach to loess/paleosol sequences from Bohemia and Moravia (Czech Republic): Implications for the Upper Pleistocene paleoenvironment in central Europe. *Palaeogeography, Palaeoclimatology, Palaeoecology*, 418, pp. 344–358.
29. Hošek, J., Hambach, U., Lisá, L., Matys G. T., Horáček, I., 2015, an integrated rock-magnetic and geochemical approach to loess/paleosol sequences from Bohemia and Moravia (Czech Republic): Implications for the Upper Pleistocene paleoenvironment in central Europe. *Palaeogeography, Palaeoclimatology, Palaeoecology* 418, 344–358.
30. Huang, G., Liu, J., Zhang, L., & Zhang, X. (2022). Magnetic susceptibility of loess deposits as a proxy for paleoenvironmental changes: Implications for climate variations in North China. *Journal of Quaternary Science*, 37(5), 639–652.
31. Jary, Z., Ciszek, D., 2013. Late Pleistocene loess–paleosol sequences in Poland and western Ukraine. *Quat. Int.* 296, 37–50.
32. Jiang, Y., et al. (2020). "Soil organic carbon dynamics in response to climate change: A review." *Global Change Biology*, 26(5), 1–16.
33. Jordanova D, Jordanova N, 2024, Geochemical and mineral magnetic footprints of provenance, weathering and pedogenesis of loess and paleosols from North Bulgaria. *Catena*, Volume 243, 108131.
34. Jordanova, D., Grygar, T., Jordanova, N., Petrov, P., 2011. Palaeoclimatic significance of hematite/goethite ratio in Bulgarian loess–paleosol sediments deduced by DRS and rock magnetic measurements. In: Petrovsky, E., Ivers, D., Harinarayana, T., Herrero- Bervera, E. (Eds.), the Earth's Magnetic Interior. IAGA Special Sopron Book Series. SpringerVerlag, Berlin.

Formatted: Indent: Hanging: 0.25"

35. Karimi, A., Khademi, H., Ayoubi, A., 2013, Magnetic susceptibility and morphological characteristics of a loess–paleosol sequence in northeastern Iran, *Catena*, 101, pp. 56-60.
36. Karimi, A., Khademi, H., Jalalian, A., 2011, Loess: Characterize and application for paleoclimate study, *Geography Research*, Volume 76, pp1-20.
37. Karimi, A., Khademi, H., Kehl, M., Jalaian, A., 2009, Distribution, Lithology and Provenance of Peridesert Loess Deposits in Northeast Iran, *Geoderm*, No.148, pp. 241250.
38. Kehl, M., Frechen, M., Skowronek, A., 2005, Paleosols Derived from Loess and Loesslike Sediments in the Basin of Persepolis, Southern Iran, *Quaternary International*, No.140/141, pp.135-149.
39. Kehl, M., Sarvati, R., Ahmadi, H., Frechen, M., Skowronek, A., 2006, Loess / Paleosol sequences along a Climatic Gradient in Northern Iran, *Eiszeitalter und Gegenwart*, No. 55, pp.149-173.
40. Lateef, A.S.A., 1988. Distribution, provenance, age and paleoclimatic record of the loess in Central North Iran. In: Eden, D.N., Furrer, R.J. (Eds.), *Loess – its Distribution, Geology and Soil*. Proceeding of an International Symposium on Loess, New Zealand, 14–21 February 1987. Balkema, Rotterdam, pp. 93–101.
41. Makeev A., Rusakov A., Kust P., Lebedeva M., Khokhlova O., 2024, Loess-paleosol sequence and environmental trends during the MIS5 at the southern margin of the Middle Russian Upland, *Quaternary Science Reviews* Volume 328, 108372.
42. Mehdipour, F., 2012, Investigation of paleoclimate in late quaternary western alborz using of technical applied and magnetism parameters, *Geology and Mineral Exploration*, master science thesis.
43. Nabavi, Mehdi, 1976, *Introduction geology of Iran*, pp1-109.
44. Okhravi, R., Amini, A., 2001, Characteristics and Provenance of the Loess Deposits of the Gharatikan Watershed in Northeast Iran, *Global and Planetary Change*, No. 28, pp.11-22.
45. Pashaei, A., 1996, Study of Chemical and Physical and Origin of Loess Deposits in Gorgan and Dasht Area, *Earth Science*, 23/24, pp. 67-78.
46. Prins, M.A., Vriend, M., Nugteren, G., Vandenberghe, J., Huazu, L., Zheng, H., Weltje, G.J., 2007, Late Quaternary aeolian dust input variability on the Chinese Loess Plateau: inference from unmixing of loess grain-size record. *Quaternary Science Reviews* 26, 230– 242.
47. Schatz, A.-K., Scholten, T., Kühn, P., 2014. Paleoclimate and weathering of the Tokaj (NE Hungary) loess–paleosol sequence: a comparison of geochemical weathering indices and paleoclimate parameters. *Clim. Past Discuss.* 10, 469–507.
48. Song, Y., Shi, Z., Dong, H., Nie, J., Qian, L., Chang, H. & Qiang, X., 2008- Loess Magnetic Susceptibility in Central Asia and its Paleoclimatic Significance. *IEEE International Geoscience & Remote Sensing Symposium*, II 1227-1230, Massachusetts.
49. Spassov, S., 2002. Loess Magnetism, Environment and Climate Change on the Chinese Loess Plateau. *Doctoral Thesis, ETH Zürich*, pp. 1–151.
50. Taylor, S.R., McLennan, S.M., McCulloch, M.T., 1983. Geochemistry of loess, continental crustal composition and crustal model ages. *Geochimica et Cosmochimica Acta* 47, 1897– 1905.

51. Zhang, Q., Chang, I., & Luo, Z. (2021). Response of vegetation to climate change over the past millennium in Eurasia. *Climate Dynamics*, 56(1), 75-88.
52. Zhang, X., et al. (2021). "Using Rb/Sr ratios to assess weathering intensity in loess profiles." *Earth Surface Processes and Landforms*, 46(12), 2454-2466.
53. Zhu, K., et al. (2021). "Leaching of soil nutrients under different climate scenarios." *Journal of Geophysical Research: Biogeosciences*, 126(7).
1. Ahmad, I., Chandra, R., 2013, Geochemistry of loess paleosol sediments of Kashmir Valley, India: Provenance and weathering, *Journal of Asian Earth Sciences* 66, 73-89.
2. Antoine, P., Rousseau, D.D., Degeai, J.P., Moine, O., Lacroix, O., Kreutzer, S., Fuchs, M., Hatte, C.H., Gauthier, C., Svoboda, J. and Lisa, I., 2013, High resolution record of the environmental response to climatic variations during the Last Interglacial–Glacial cycle in Central Europe: the loess palaeosol sequence of Dolní Věstonice (Czech Republic), *Quaternary Science Reviews*, 67, pp 17–38.
3. Arias Ortiz, A., et al. (2020). "The impact of climate change on soil chemistry and biogeochemical cycles." *Nature Reviews Earth & Environment*, 1(12), 689–702.
4. Bader N E, Broze E A, Coates M A, Elliott M M, McGann G E, Strozzyk S, Burmester R F, 2024, The usefulness of the magnetic susceptibility of loess paleosol sequences for paleoclimate and stratigraphic studies: The case of the Quaternary Palouse loess, northwestern United States, *Quaternary International*, Article in Press.
5. Bai, Y., et al. (2022). "Rb/Sr ratio as a proxy for weathering and soil formation in the Loess Plateau, China." *Geoderma*, 410, 115754.
6. Baumgart, P., Hambach, U., Meszner, S., Faust, D., 2013. An environmental magnetic fingerprint of periglacial loess: records of Late Pleistocene loess paleosol sequences from Eastern Germany. *Quat. Int.* 296, 82–93.
7. Bloemendal J, Liu X, Sun Y, Li N, 2008, An assessment of magnetic and geochemical indicators of weathering and pedogenesis at two contrasting sites on the Chinese Loess plateau, *Palaeogeography, Palaeoclimatology, Palaeoecology* 257 (2008) 152–168.
8. Bloemendal, J., Xiuming L., Youbin, S., Ningning L., 2008. An assessment of magnetic and geochemical indicators of weathering and pedogenesis at two contrasting sites on the Chinese Loess plateau, *Palaeogeography, Palaeoclimatology, Palaeoecology* 257; 152–168.
9. Bronger, A., 2003. Correlation of loess paleosol sequence in East and Central Asia with SE Central Europe: toward a continental Quaternary pedomorphology and paleoclimate history. *Quaternary International* 106/107, 11–31.
10. Buggle, B., Hambach, U., Glaser, B., Gerasimenko, N., Markovic, S., Glaser, I., Zöller, L., 2009. Stratigraphy, and spatial and temporal paleoclimatic trends in Southeastern/Eastern European loess paleosol sequences. *Quat. Int.* 196, 186–206.
11. Chen, J., An, Z.S., Head, J., 1999. Variation of Rb/Sr ratios in the loess paleosol sequences of central China during the last 130,000 years and their implications for monsoon paleoclimatology. *Quaternary Research* 51, 215–219.
12. Chen, T., Xie, Q., Xu, H., Chen, J., Ji, J., Lu, J., Lu, H and Balsam, W, 2010, Characteristics and formation mechanism of pedogenic hematite in Quaternary Chinese loess and paleosols, *Catena* 81, 217–225.

Formatted: Indent: Hanging: 0.25"

13. Chlachula, J., Little, E., 2011. A high-resolution Late Quaternary climatostratigraphic record from Iskitim, Priobie Loess Plateau, SW Siberia. *Quaternary International* 240, 139e149.
14. Ding, Z.L., Ranov, V., Yang, S.L., Finaev, A., Han, J.M., Wang, G.A., 2002. The loess record in southern Tajikistan and correlation with Chinese loess. *Earth and Planetary Science Letters* 200, 387e400.
15. Ding, Z.L., Yang, S.L., Sun, J.M., Liu, T.S., 2001. Iron geochemistry of loess and Red Clay deposits in the Chinese Loess Plateau and implications for long term Asian monsoon evolution in the last 7.0 Ma. *Earth and Planetary Science Letters* 185, 99–109.
16. Fischer, P., Hilgers, A., Protze, J., Kels, H., Lehmkuhl, F., Gerlach, R., 2012. Formation and geochronology of Last Interglacial to Lower Weichselian loess/paleosol sequences—case studies from the Lower Rhine Embayment, Germany. *E & G Quat. Sci. J.* 61, 48–63.
17. Fitzsimmons, K.E., Marković, S.B., Hambach, U., 2012. Pleistocene environmental dynamics recorded in the loess of the middle and lower Danube Basin. *Quat. Sci. Rev.* 41, 104–118.
18. Forster, T., Evans, M.E., Havlíček, P., Heller, F., 1996. Loess in the Czech Republic: magnetic properties and paleoclimate. *Stud. Geophys. Geod.* 40, 243–261.
19. Frechen, M., Kehl, M., Rolf, C., Sarvati, R., Skowronek A., 2009. Loess Chronology of the Caspian Lowland in Northern Iran. *Quaternary International*, No. 198, pp. 220–233.
20. Frechen, M., Oches, E.A., Kohfeld, K.E., 2003. Loess in Europe—mass accumulation rates during the Last Glacial Period. *Quaternary Science Reviews* 22, 1835–1875.
21. Gallet, S., Jahn, B.M., Torii, M., 1996. Geochemical characterization of the Luoichuan loess-paleosol sequence, China, and paleoclimatic implications. *Chemical Geology* 133, 67–88.
22. Goeke, M., Hambach, U., Eckmeier, E., Schwark, L., Zöller, L., Fuchs, M., Löscher, M., Wiesenberg, G.L.B., 2014. Introducing an improved multi-proxy approach for paleoenvironmental reconstruction of loess-paleosol archives applied on the Late Pleistocene Nussloch sequence (SW-Germany). *Palaeogeogr. Palaeoclimatol. Palaeoecol.* 410, 300–315.
23. Guanhua, L., Dunsheng, X., Ming, J., Jia, J., Jiabo, L., Shuang, Z., Yanglei, W., 2014. Magnetic characteristics of loess-paleosol sequences in Tacheng, northwestern China, and their paleoenvironmental implications. *Quaternary International*, 3, 1–10.
24. Guo, Z.T., Ruddiman, W.F., Hao, Q.Z., Wu, H.B., Qiao, Y.S., Zhu, R.X., Peng, S.Z., Wei, J.J., Yuan, B.Y., and Liu, T.S., 2002. Onset of Asian desertification by 22 Myr ago inferred from loess deposit in China. *Nature* Vol. 416, pp. 159–163.
25. Heller, F., Liu, T., 1984. Magnetism of Chinese loess deposits. *Geophys. J. R. Astron. Soc.* 77, 125–141.
26. Hosek J., Hambach U., Lisa L., Grygar T.M., Horacek I., Meszner S., Knesl I., 2015. An integrated rock-magnetic and geochemical approach to loess/paleosol sequences from Bohemia and Moravia (Czech Republic): Implications for the Upper Pleistocene paleoenvironment in central Europe. *Palaeogeography, Palaeoclimatology, Palaeoecology*, 418, pp. 344–358.

27. Hošek, J., Hambach, U., Lisá, L., Matys G. T., Horáček, I., 2015, an integrated rock-magnetic and geochemical approach to loess/paleosol sequences from Bohemia and Moravia (Czech Republic): Implications for the Upper Pleistocene paleoenvironment in central Europe, *Palaeogeography, Palaeoclimatology, Palaeoecology* 418, 344–358.
28. Jary, Z., Ciszek, D., 2013. Late-Pleistocene loess-paleosol sequences in Poland and western Ukraine. *Quat. Int.* 296, 37–50.
29. Jiang, Y., et al. (2020). "Soil organic carbon dynamics in response to climate change: A review." *Global Change Biology*, 26(5), 1–16.
30. Jordanova D., Jordanova N., 2024, Geochemical and mineral magnetic footprints of provenance, weathering and pedogenesis of loess and paleosols from North Bulgaria, *Catena*, Volume 243, 108131.
31. Jordanova, D., Grygar, T., Jordanova, N., Petrov, P., 2011. Palaeoclimatic significance of hematite/goethite ratio in Bulgarian loess-paleosol sediments deduced by DRS and rock magnetic measurements. In: Petrovsky, E., Ivers, D., Harinarayana, T., Herrero-Bervera, E. (Eds.), *the Earth's Magnetic Interior. IAGA Special Sopron Book Series*. Springer-Verlag, Berlin.
32. Karimi, A., Khademi, H., Ayoubi, A., 2013, Magnetic susceptibility and morphological characteristics of a loess-paleosol sequence in northeastern Iran, *Catena*, 101, pp. 56–60.
33. Karimi, A., Khademi, H., Jalalian, A., 2011, Loess: Characterize and application for paleoclimate study, *Geography Research*, Volume 76, pp. 1–20.
34. Karimi, A., Khademi, H., Kehl, M., Jalalian, A., 2009, Distribution, Lithology and Provenance of Peridesert Loess Deposits in Northeast Iran, *Geoderma*, No. 148, pp. 241–250.
35. Kehl, M., Frechen, M., Skowronek, A., 2005, Paleosols Derived from Loess and Loesslike Sediments in the Basin of Persepolis, Southern Iran, *Quaternary International*, No. 140/141, pp. 135–149.
36. Kehl, M., Sarvati, R., Ahmadi, H., Frechen, M., Skowronek, A., 2006, Loess/Paleosol sequences along a Climatic Gradient in Northern Iran, *Eiszeitalter und Gegenwart*, No. 55, pp. 149–173.
37. Lateef, A.S.A., 1988. Distribution, provenance, age and paleoclimatic record of the loess in Central North Iran. In: Eden, D.N., Furrkert, R.J. (Eds.), *Loess—its Distribution, Geology and Soil. Proceeding of an International Symposium on Loess*, New Zealand, 14–21 February 1987. Balkema, Rotterdam, pp. 93–101.
38. Makeev A., Rusakov A., Kust P., Lebedeva M., Khokhlova O., 2024, Loess-paleosol sequence and environmental trends during the MIS5 at the southern margin of the Middle Russian Upland, *Quaternary Science Reviews* Volume 328, 108372.
39. Mehdipour, F., 2012, Investigation of paleoclimate in late quaternary western alborz using of technical applied and magnetism parameters, *Geology and Mineral Exploration*, master science thesis.
40. Nabavi, Mehdi, 1976, Introduction geology of Iran, pp. 1–109.
41. Okhravi, R., Amini, A., 2001, Characteristics and Provenance of the Loess Deposits of the Gharatikan Watershed in Northeast Iran, *Global and Planetary Change*, No. 28, pp. 11–22.
42. Pashaei, A., 1996, Study of Chemical and Physical and Origin of Loess Deposits in Gorgan and Dasht Area, *Earth Science*, 23/24, pp. 67–78.

43. Prins, M.A., Vriend, M., Nugteren, G., Vandenberghe, J., Huazu, L., Zheng, H., Weltje, G.J., 2007. Late Quaternary aeolian dust input variability on the Chinese Loess Plateau: inference from unmixing of loess grain size record. *Quaternary Science Reviews* 26, 230–242.
44. Schatz, A. K., Scholten, T., Kühn, P., 2014. Paleoclimate and weathering of the Tokaj (NE Hungary) loess–paleosol sequence: a comparison of geochemical weathering indices and paleoclimate parameters. *Clim. Past Discuss.* 10, 469–507.
45. Song, Y., Shi, Z., Dong, H., Nie, J., Qian, L., Chang, H. & Qiang, X., 2008. Loess Magnetic Susceptibility in Central Asia and its Paleoclimatic Significance. *IEEE International Geoscience & Remote Sensing Symposium, II* 1227–1230, Massachusetts.
46. Spassov, S., 2002. Loess Magnetism, Environment and Climate Change on the Chinese Loess Plateau. Doctoral Thesis, ETH Zürich, pp. 1–151.
47. Taylor, S.R., McLennan, S.M., McCulloch, M.T., 1983. Geochemistry of loess, eontinental crustal composition and crustal model ages. *Geochimica et Cosmochimica Acta* 47, 1897–1905.
48. Zhang, X., et al. (2021). "Using Rb/Sr ratios to assess weathering intensity in loess profiles." *Earth Surface Processes and Landforms*, 46(12), 2454–2466.
49. Zhu, K., et al. (2021). "Leaching of soil nutrients under different climate scenarios." *Journal of Geophysical Research: Biogeosciences*, 126(7).
50. Huang, G., Liu, J., Zhang, L., & Zhang, X. (2022). Magnetic susceptibility of loess deposits as a proxy for paleoenvironmental changes: Implications for climate variations in North China. *Journal of Quaternary Science*, 37(5), 639–652.

Formatted: No bullets or numbering